Chemical and Process Engineering: New Frontiers, 2023, 44(2), e11
DOI: 10.24425/cpe.2023.144697

Axial thrust in a vessel with unsteady rotating axial impeller

Szymon Woziwodzki*

Poznan University of Technology, Department of Chemical Engineering and Equipment, Berdychowo 4, 60-965 Poznan, Poland

* **Corresponding author:**
e-mail:
szymon.woziwodzki@put.poznan.pl

Presented at 24th Polish Conference of Chemical and Process Engineering, 13–16 June 2023, Szczecin, Poland.

Article info:
Received: 28 April 2023
Revised: 07 June 2023
Accepted: 29 June 2023

Abstract
Unsteady motion of the impeller is one of many methods to improve mixing in an unbaffled vessel. It is very important in pharmaceutical industry, crystallization processes or some chemical reactions with catalyst where baffles are not recommended. The literature data shows that unsteady mixing causes generation of axial flow for radial impellers (Rushton turbine). The purpose of this study was to investigate axial force for axial impellers like A315, HE-3 and SC-3. Moreover, the momentum number, flow number and pumping efficiency were analysed. Results show that axial force for unsteady mixing was higher in comparison to steady-state mixing. Also, the comparison of axial force between impellers shows that blades influence momentum number and flow number. Impellers with larger blade surface generate stronger axial force. The obtained results reveal that unsteady mixing with axial impellers could be applied for solid-liquid mixing as a suitable alternative to steady-state mixing.

Keywords
unsteady mixing, axial force, oscillations, axial thrust, axial impellers

1. INTRODUCTION

Unsteady mixing is one of the methods to improve mixing is unbaffled vessels. It is very important in pharmaceutical industry where cleaning issues play an important role. When baffles are removed, power requirement drop is observed because of the strong circumferential flow (primary flow) and central vortexing (Kamieński, 2004; Paul et al., 2004; Stręk, 1981) which result in poor mixing. Unsteady mixing could be achieved in several ways, such as reciprocating motion of the impeller (Komoda et al., 2019; Masiuk et al., 2008; Ni et al., 2003; Wójtowicz, 2017) or unsteady rotation of the impeller (Frankiewicz and Woziwodzki, 2022; Yoshida et al., 2012). It could be applied to improve the mixing of liquid-liquid, gas-liquid, and solid-liquid mixtures of Newtonian fluids as a well as non-Newtonian ones.

The hydrodynamics of unsteady mixing is complex. This consists of several aspects, such as the effect of liquid inertia and the delay of the change in the direction of circulation of the liquid relative to the change in the direction of rotation of the impeller, the formation of vortices behind the impeller blades, and the creation of areas of flow disturbances.

Roy and Acharya, (2011; 2012) shows that for radial impellers, two circulation loops are generated during unsteady mixing. At the moment of the highest impeller speed N_{max}, the radial impeller generates a strong stream of liquid leaving the impeller zone towards the vessel wall. When the impeller decelerates, then the stream leaving the impeller zone is additionally affected by upper circulation loop with a force corresponding to the maximum speed N_{max}. This causes the radial stream to deflect towards the bottom of the vessel. With a further reduction in the impeller speed, this stream loses its radial force in favour of a stronger axial flow directed towards the bottom of the vessel. During deceleration, a decrease in radial velocity and an increase in axial and circumferential velocity are observed. For this reason, the radial impeller generates an axial flow that does not occur in a standard stirred vessel. Studies by (Yoshida et al., 2008; 2010) confirm that the use of unsteady mixing promotes an increase in axial force and pumping capacity for radial impellers. The increase is about 13% for unsteady mixing with a change of direction of rotation and from 3% to 56% for unsteady mixing with a constant direction of rotation.

Yoshida et al. (2012) and Tezura et al., (2007; 2008) conducted analysis of solid-liquid unsteady mixing. Tezura et al. (2007) investigated the effect of unsteady mixing in unbaffled vessel on just-suspended impeller speed and mixing power. It has been shown that the circumferential flow in the zone below the impeller is minimized. It suggests that unsteady mixing could be an effective method to reach off-bottom suspension with less power requirements in comparison to steady-state mixing. Tezura et al. (2008) found unsteady mixing caused reduction of gas surface aeration and sufficient solid-liquid contact. They also investigated solid-liquid mass transfer and found that mass transfer coefficients $k_L a$ for unsteady mixing were comparable with $k_L a$ coefficients for steady mixing (baffled vessel). Yoshida et al. (2012) investigated an effect of unsteady mixing on minimum impeller speed for complete dispersion. They found that unsteady motion improved turbulence for radial impellers. Moreover, they proposed correlations for complete dispersion impeller speed and determined the values of the Zwietering constants.

The aim of this work was to analyse the axial force for pitched blade impellers and to evaluate the use of axial impellers for solid-liquid unsteady mixing.

2. EXPERIMENTAL PART

2.1. Experimental set-up and methods

The experimental set-up is presented at Fig. 1. It consists of motor (1), inverter (2), PC computer (4), vessel (5), impeller (6) and balance (7). A flat bottomed, unbaffled vessel of diameter $T = 0.29$ m was equipped with a single impeller with a diameter of $D = 0.1$ m. The impeller bottom clearance was $C = 0.1$ m ($C/D = 1$) and the liquid height was the same as vessel diameter ($H = T$).

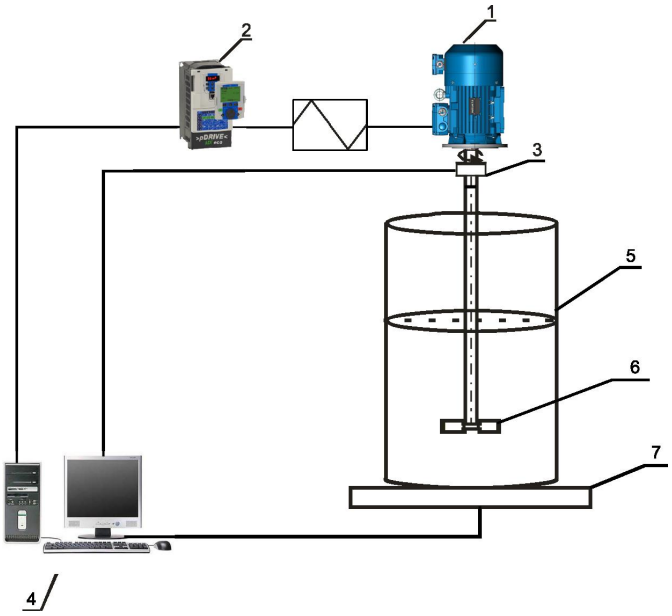

Figure 1. Experimental setup: 1 – motor, 2 – inverter, 3 – torquemeter, 4 – PC, 5 – vessel, 6 – impeller, 7 – balance.

Three different impellers with pitched blade were used: SC-3, HE-3 and A315 (Figure 2).

Impeller speed, N, was changing with time, t, according to triangle time-course (Woziwodzki, 2011) described by Eq. (1)

$$N = \frac{8}{\pi^2} N_{\max} \left(\sin(2\pi f t) - \frac{1}{9} \sin(6\pi f t) + \frac{1}{25} \sin(10\pi f t) \right) \quad (1)$$

where $N_{\max}$ and f are maximum impeller speed and oscillation frequency.

Maximum impeller speed was changed from $N_{\max} = 4$ 1/s up to $N_{\max} = 12$ 1/s within the turbulent flow regime and

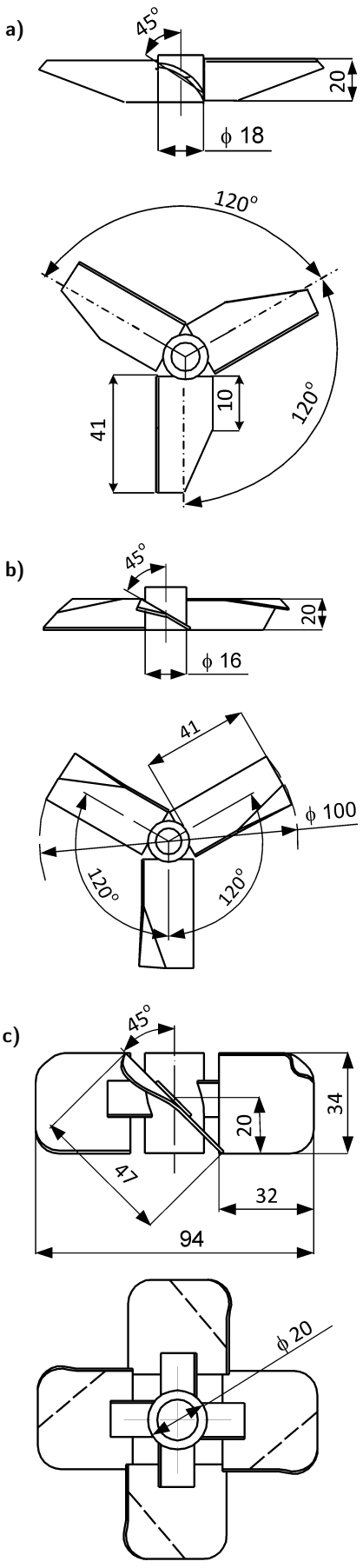

Figure 2. Impellers: a) SC-3, b) HE-3, c) A315.

oscillation frequency, f, from 0.115 Hz to 0.46 Hz. Time-course of impeller speed and oscillation frequency were set by inverter Schneider MX Eco and internal waveform generator (Woziwodzki, 2011). As a working fluid water was used of a temperature of 20 °C.

In order to determine the axial force generated by the impeller, the method proposed by Fořt et al. (2013) was used, which consists in measuring the axial pressure on the bottom of the vessel. The axial thrust was determined with the weight method. It is usually represented as axial thrust number Th or as momentum number Mo (Eq. (2)).

$$Th = \mathrm{Mo} = \frac{F_a}{N^2 D^4 \rho} \tag{2}$$

where F_a is axial force.

The use of axial momentum is convenient, because unlike the volumetric flow rate it is constant (Fořt et al., 2008; Fořt, 2011; Jones et al., 2009). The momentum balance is carried out by integrating the cylindrical volume around the impeller (Machado et al., 2012) and is proportional to the flow number ($\mathrm{Fl} = Q/ND^3$) squared

$$\mathrm{Mo} = \frac{9}{2\pi}\mathrm{Fl}^2 \tag{3}$$

and

$$\mathrm{Fl} = \left(\frac{\mathrm{Mo}}{1.43}\right)^{0.5} \tag{4}$$

Machado et al. (2012) also proposed another value for the constant in Equation (5): 1.45 and 1.46 respectively. In further calculations 1.43 constant was used according to Eq. (4). Due to the measurement limitations of the balance, the tests were carried out in the range of Keulegan–Carpenter KC > 15.

$$\mathrm{KC} = \frac{N_{\max}}{f} \tag{5}$$

where $N_{\max}$ is maximum impeller speed and f is oscillation frequency.

2.2. Results

Figure 3 shows typical relation between axial force and Keulegan–Carpenter number for all impellers. For unsteady mixing during changes in the impeller speed, two directions of axial force were observed, which is associated with a change in the direction of pumping the liquid through the impeller. When pumping liquid towards the bottom of the vessel, higher axial force values are obtained than for pumping the liquid upwards. The greatest differences of upward and downward axial force were observed for SC-3 (about 2.4 times) impeller while for A315 the smallest (about 20%).

The differences in axial force were related to the shape and area of blades. A315 impeller has the greatest blade area, while SC-3 impeller blade is concave or convex depending on the direction of rotation. When impeller rotates in clockwise-direction, blade surface is concave, and downward pumping is

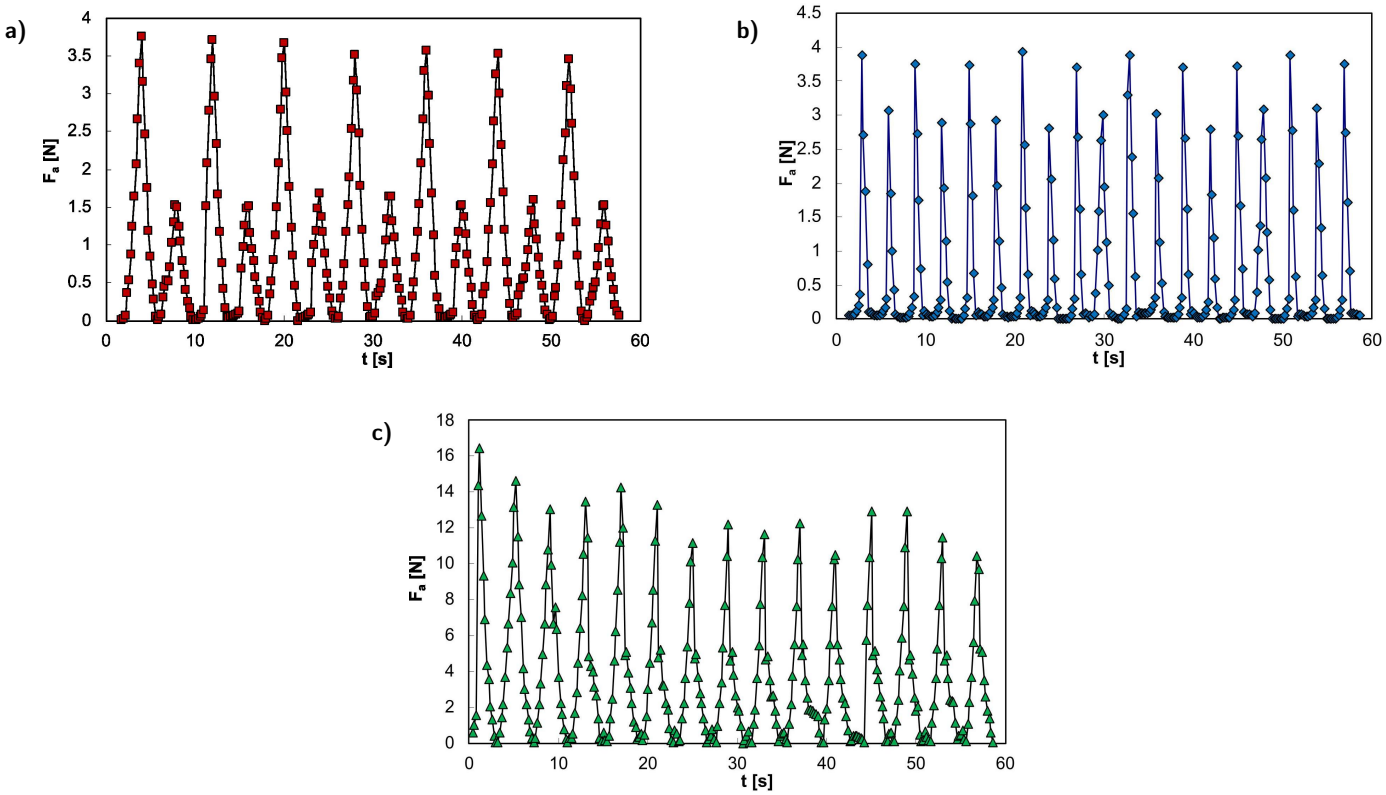

Figure 3. Time course of axial force: a) SC-3, KC = 81, b) HE-3, KC = 21, c) A315, KC = 19.

achieved, while for counter-clockwise direction blade is convex, and upward circulation is observed.

The momentum number Mo is defined by Equation (2). Since in the range of KC > 15 the drag force is dominant, the maximum impeller speed was used in the definition of the number Mo. The Mo number is constant and independent of the Reynolds and Keulegan–Carpenter numbers (for Re > 10000 and KC > 15). Figure 4 shows the relationship between the Mo number and the KC number for all impellers evaluated. Based on the literature data, the value of the momentum number Mo was determined for the A315, HE-3 and SC-3 impellers during steady-state mixing. For the A315 impeller, the momentum number was Mo = 0.804 (Bakker, 1992), for the HE-3 impeller Mo = 0.343–0.358 (Coker, 2007), and for the SC-3 impeller Mo = 0.426 (Michalak, 2015).

Table 1. Comparison of Mo and Fl values for unsteady and steady-state mixing.

Impeller	Unsteady mixing		Steady-state mixing	
	Mo	Fl	Mo	Fl
A315	1.106	0.88	0.804 (Bakker, 1992)	0.74 (Bakker, 1992)
HE-3	0.550	0.620	0.343–0.358 (Coker, 2007)	0.41 (Coker, 2007)
SC-3	0.429	0.548	0.426 (Michalak, 2015)	0.546 (Michalak, 2015)

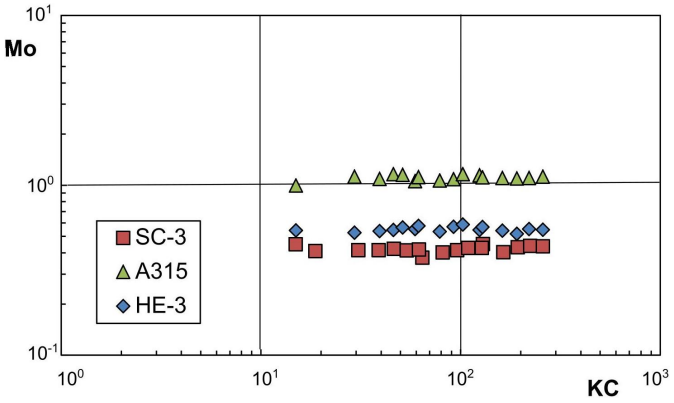

Figure 4. Relation between momentum number Mo and Keulegan–Carpenter number KC.

Experimental results confirm Mo number is independent of oscillation frequency and within turbulent flow regime and KC > 15 is constant. The greatest value was obtained for A315 impeller (Mo = 1.106). The momentum number for HE-3 was about 50% smaller (Mo = 0.55) and 62% for SC-3 (Mo = 0.429). The comparison with momentum number for steady-state mixing reveals that axial thrust for unsteady mixing is greater, 37% for A315, 53%–60% for HE-3. Only for SC-3, the difference was negligible.

In the last step the calculation of the flow number Fl was performed. Flow number is crucial in description of hydrodynamics and circulation generated by impellers and is defined by Eq. (6)

$$\mathrm{Fl} = \frac{Q}{ND^3} \tag{6}$$

Within turbulent flow regime, flow number is independent of Reynolds number. Such relationship is valid for steady-state and unsteady mixing. Figure 5 presents the effect of oscillation frequency on Fl. It shows that Fl number, like Mo number, within turbulent flow regime is independent of oscillation frequency and Keulegan–Carpenter number. For A315 impeller, flow number was Fl = 0.88, for HE-3 Fl = 0.62 and for SC-3 Fl = 0.54. Flow numbers for unsteady mixing were greater in comparison to steady-state mixing. Results suggest that unsteady mixing could be recommended for solid-liquid systems.

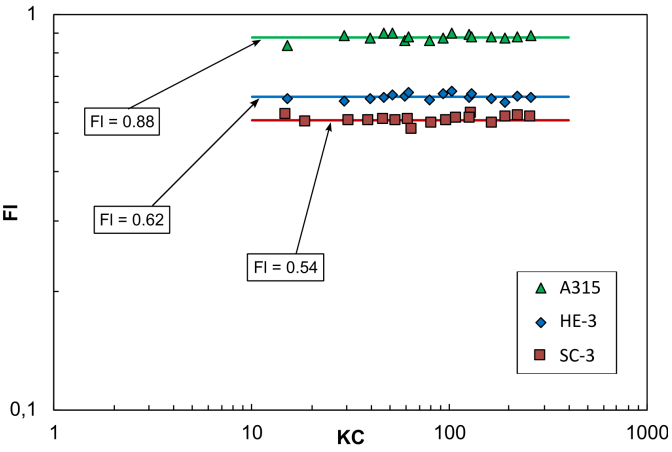

Figure 5. Effect of oscillation frequency on flow number Fl.

The highest Mo values were obtained for the A315 impeller, which has the largest blade projection surface. It is about 2.8 times larger than the other impellers, while the Mo number is up to 2.5 times greater. This means that the A315 has the smallest pressure difference on the impeller blade, it is about 20% less than for the HE-3 agitator and 13% for the SC-3.

In the next step, hydraulic efficiency was considered. The hydraulic efficiency E_p of the impeller determines the ability to convert the energy of the impeller into pumping capacity. It could be determined based on flow number Fl and Newton number Ne.

$$E_p = \frac{\mathrm{Fl}^3}{\mathrm{Ne}} \left(\frac{D}{T}\right)^4 \tag{7}$$

Mixing power was calculated from Eq.(8) using methodology proposed by Yoshida et al. (1999).

$$P = 2\pi N_{\mathrm{av}} M_{\mathrm{av}} \tag{8}$$

where N_{av} is integral mean impellers speed (obtained from Eq. (1)) and M_{av} integral mean torque obtained from the Morison equation (Woziwodzki, 2020).

The Newton number for unsteady mixing and turbulent flow regime is independent of KC number (KC $>$ 15) and for A315, HE-3 and SC-3 impellers is as follows: $Ne_{A315} = 2.98$, $Ne_{HE-3} = 1.49$ and $Ne_{SC-3} = 0.88$. My own research indicates unsteady mixing power is about 33%–50% greater (Woziwodzki, 2011) in comparison to steady-state mixing.

The higher E_p value, the greater pumping ability. The experimental results obtained indicate that during unsteady mixing, the A315 impeller achieved the highest hydraulic efficiency. The efficiency E_p was 0.00324. For the HE-3 impeller, the hydraulic efficiency was reduced by 30% ($E_p = 0.00226$). The SC-3 agitator achieved the highest hydraulic efficiency compared to the HE-3 impeller ($E_p = 0.00264$)

3. CONCLUSIONS

The paper presents results of a study of axial force in a vessel with unsteady rotating axial impeller. The axial force, momentum number, flow number and pumping efficiency were analysed. The results show that blade area has the greatest effect on axial force. That is why the momentum number and flow number are highest for A315 impeller. For three bladed impellers (HE-3 and SC-3) the axial force for the first impeller was higher. It was due to the fact that HE-3 impeller had flat blades while SC-3 impeller concave and convex blades dependent on direction of rotation. However, the pumping efficiency of SC-3 impeller was better than that of HE-3. The highest pumping efficiency was achieved for A315 impeller.

The comparison of axial mixing and flow numbers for unsteady and steady-state mixing reveal that unsteady mixing could be recommended for solid-liquid systems when the use of baffles is not recommended.

ACKNOWLEDGEMENTS

This research was founded by Ministry of Education and Science.

SYMBOLS

C	impeller bottom clearance, m
D	impeller diameter, m
f	oscillation frequency, Hz
F_a	axial force, N
Fl	impeller flow number, $Fl = Q/(ND^3)$
H	liquid height, m
k_La	volumetric mass transfer coefficient, 1/s
KC	Keulegan–Carpenter number, $KC = N_{max}/f$
M_{av}	integral mean torque, Nm
N	impeller speed, 1/s
N_{av}	integral average impeller speed, 1/s
N_{max}	maximum impeller speed, 1/s
Ne	Newton number for unsteady mixing, $Ne = P/(N_{av}^3 D^5 \rho)$
Q	impeller volumetric flow rate, m^3/s
P	mixing power, W
Re	Reynolds number for unsteady mixing, $Re = N_{av} D^2 \rho/\eta$
t	time, s
T	vessel diameter, m
η	dynamic viscosity, Pa·s
ρ	density, kg/m^3

REFERENCES

Bakker A., 1992. *Hydrodynamics of stirred gas-liquid dispersions*. Ph.D. Dissertation, February 1992, Delft University of Technology, Delft, The Netherlands.

Coker A.K., 2007. Ludwig's applied process design for chemical petrochemical plants. Elsevier, Amsterdam.

Fořt I., 2011. On hydraulic efficiency of pitched blade impellers. *Chem. Eng. Res. Des.*, 89, 611–615. DOI: 10.1016/j.cherd.2010.10.005.

Fořt I., Hasal P., Paglianti A., Magelli F., 2008. Axial force at the vessel bottom induced by axial impellers. *Acta Polytech.*, 48, 45–50. DOI: 10.14311/1039.

Fořt I., Seichter P., Pešl L., 2013. Axial thrust of axial flow impellers. *Chem. Eng. Res. Des.*, 91, 789–794. DOI: 10.1016/j.cherd.2012.10.001.

Frankiewicz S., Woziwodzki S., 2022. Gas hold-up and mass transfer in a vessel with an unsteady rotating concave blade impeller. *Energies*, 15, 346. DOI: 10.3390/en15010346.

Jones P.N., Özcan-Taşkin N.G., Yianneskis M., 2009. The use of momentum ratio to evaluate the performance of CSTRs. *Chem. Eng. Res. Des.*, 87, 485–491. DOI: 10.1016/j.cherd.2008.12.005.

Kamieński J., 2004. *Mieszanie układów wielofazowych*. WNT, Warszawa.

Komoda Y., Tomimasu F., Hidema R., Suzuki H., 2019. Frequency analysis of torque variation of a rotationally reciprocating impeller using newtonian and viscoelastic fluids. *Chem. Eng. Res. Des.*, 142, 327–335. DOI: 10.1016/j.cherd.2018.12.022.

Machado M.B., Nunhez J.R., Nobes D., Kresta S.M., 2012. Impeller characterization and selection: Balancing efficient hydrodynamics with process mixing requirements. *AIChE J.*, 58, 2573–2588. DOI: 10.1002/aic.12758.

Masiuk S., Rakoczy R., Kordas M., 2008. Comparison density of maximal energy for mixing process using the same agitator in rotational and reciprocating movements. *Chem. Eng. Process. Process Intensif.*, 47, 1252–1260. DOI: 10.1016/j.cep.2007.04.004.

Michalak T. 2015. *Projekt i badania modelowe mieszadła SC-3*. Politechnika Poznańska, Poznań.

Ni X., Mackley M.R., Harvey A.P., Stonestreet P., Baird M.H.I., Rama Rao N.V., 2003. Mixing through oscillations and pulsations – a guide to achieving process enhancements in the chemical and process industries. *Chem. Eng. Res. Des.*, 81, 373–383. DOI: 10.1205/02638760360596928.

Paul E.L., Atiemo-Obeng V., Kresta S.M., 2004. *Handbook of industrial mixing: Science and practice*. John Wiley & Sons, Hoboken.

Roy S., Acharya S., 2011. Perturbed turbulent stirred tank flows with amplitude and mode-shape variations. *Chem. Eng. Sci.*, 66, 5703–5722. DOI: 10.1016/j.ces.2011.08.005.

Roy S., Acharya S., 2012. Scalar mixing in a turbulent stirred tank with pitched blade turbine: Role of impeller speed perturbation. *Chem. Eng. Res. Des.*, 90, 884–898. DOI: 10.1016/j.cherd.2011.10.009.

Stręk F., 1981. *Mieszanie i mieszalniki*. WNT, Warszawa.

Tezura S., Kimura A., Yoshida M., Yamagiwa K., Ohkawa A., 2007. Agitation requirements for complete solid suspension in an unbaffled agitated vessel with an unsteadily forward-reverse rotating impeller. *J. Chem. Technol. Biotechnol.*, 82, 672–680. DOI: 10.1002/jctb.1726.

Tezura S., Kimura A., Yoshida M., Yamagiwa K., Ohkawa A., 2008. Solid–liquid mass transfer characteristics of an unbaffled agitated vessel with an unsteadily forward–reverse rotating impeller. *J. Chem. Technol. Biotechnol.*, 83, 763–767. DOI: 10.1002/jctb.1849.

Wójtowicz R., 2017. Flow pattern and power consumption in a vibromixer. *Chem. Eng. Sci.*, 172, 622–635. DOI: 10.1016/j.ces.2017.07.010.

Woziwodzki S., 2011. Unsteady mixing characteristics in a vessel with forward-reverse rotating impeller. *Chem. Eng. Technol.*, 34, 767–774. DOI: 10.1002/ceat.201000455.

Woziwodzki S., 2020. Application of morison equation in unsteady mixing characteristics, In: Ochowiak M., Woziwodzki S., Mitkowski P.T., Doligalski M. (Eds.), *Practical aspects of chemical engineering: Selected Contributions from PAIC 2019*. Springer International Publishing AG, 491–499.

Yoshida M., Hiura T., Yamagiwa K., Ohkawa A., Tezura S., 2008. Liquid flow in impeller region of an unbaffled agitated vessel with an angularly oscillating impeller. *Can. J. Chem. Eng.*, 86, 160–167. DOI: 10.1002/cjce.20028.

Yoshida M., Kimura A., Yoneyama A., Tezura S., 2012. Design and operation of unbaffled vessels agitated with an unsteadily forward–reverse rotating impeller handling solid–liquid dispersions. Asia-Pac. *J. Chem. Eng.*, 7, 572–580. DOI: 10.1002/apj.609.

Yoshida M., Wakura Y., Yamagiwa K., Ohkawa A., Tezura S., 2010. Liquid flow circulating within an unbaffled vessel agitated with an unsteady forward-reverse rotating impeller. *J. Chem. Technol. Biotechnol.*, 85, 1017–1022. DOI: 10.1002/jctb.2353.

Yoshida M., Yamagiwa K., Ohkawa A., Takahashi K., Shimazaki M., Abe M., 1999. Torque of drive shaft with unsteadily rotating impellers in an unbaffled aerated agitation vessel. *Mat. Technol.*, 17, 19–31.